Scientific paper

Syntheses, Crystal Structures and Antimicrobial Activity of Ni^{II}, Zn^{II} and Mn^{III} Complexes Derived from *N*,*N*'-Bis(4-bromosalicylidene)propane-1,2-diamine

Yu-Mei Hao

Laboratory of Clean Energy in Western Jilin Province, Baicheng Normal University, Baicheng 137000, P.R. China

* Corresponding author: E-mail: jyxygzb@163.com

Received: 12-19-2024

Abstract

Four new nickel(II), zinc(II) and manganese(III) complexes, [NiL] (1), [Zn₃L₂(OAc)₂] (2), [ZnL(CH₃OH)] (3) and [Mn-ClL(DMF)] (4), derived from the bis-Schiff base *N*,*N*'-bis(4-bromosalicylidene)propane-1,2-diamine (H₂L) have been prepared and characterized by spectroscopy methods, as well as single crystal X-ray determination. The Ni atom in the mononuclear nickel complex 1 is in square planar coordination. The outer and inner Zn atoms in the trinuclear zinc complex 2 are in square planar and octahedral coordination, respectively. The Zn atom in the mononuclear zinc complex 3 is in square pyramidal coordination. The Mn atom in the mononuclear manganese complex 4 is in octahedral coordination. Antibacterial activity of the complexes has been assayed on the bacteria *Staphylococcus aureus* and *Escherichia coli*, and the yeast *Candida parapsilosis*.

Keywords: Schiff base; Nickel complex; Zinc complex; Manganese complex; Antibacterial activity

1. Introduction

Schiff bases have been extensively used as organic ligands in coordination chemistry for their facile synthesis and metal-binding capability. Compounds bearing O, N and S atoms are structurally similar with some natural biological enzymes. Schiff bases and their complexes with transition metal ions have interesting biological and pharmaceutical applications. In the last few decades, Schiff bases have shown great biological activities like antibacterial, antifungal, anti-proliferative, antiviral, antimalarial, anti-inflammatory and antipyretic. A number of nickel,

N N N OH HO Br

Scheme 1. H₂L

zinc and manganese complexes with Schiff base ligands have been reported, and most of the complexes show effective antibacterial activities. However, the relationship between structures of complexes and their properties is unclear, it is necessary to study new samples to find more effective agents and to better understand the biological mechanisms. In this work, four new nickel(II), zinc(II) and manganese(III) complexes, [NiL] (1), [Zn₃L₂(OAc)₂] (2), [ZnL(CH₃OH)] (3) and [MnClL(DMF)] (4), where L is the dianionic form of the bis-Schiff base *N*,*N*'-bis(4-bromosalicylidene)propane-1,2-diamine (H₂L; Scheme 1), are presented.

2. Experimental

2. 1. Materials and Methods

4-Bromosalicylaldehyde and 1,2-diaminopropane were purchased from TCI Chemical Reagent Co. Ltd. Zinc acetate, zinc chloride and manganese chloride were purchased from Aladdin Chemical Reagent Co. Ltd. Methanol and DMF were purchased from Kemiou Chemical Reagent Co. Ltd. The Schiff base $\rm H_2L$ was synthesized according to literature method. Elemental analyses were performed on a Perkin-Elmer 240C elemental analyzer. IR

spectra were recorded on a Jasco FT/IR-4000 spectrometer as KBr pellets in the 4000–400 cm⁻¹ region. UV-Vis spectra were recorded on a Lambda 900 spectrometer. Single crystal X-ray diffraction was carried out on a Bruker SMART 1000 CCD diffractometer.

2. 2. Synthesis of the Complexes

2. 2. 1. [NiL] (1)

 $\rm H_2L$ (44 mg, 0.10 mmol) and NiCl₂·6H₂O (48 mg, 0.20 mmol) were dissolved in methanol (30 mL). The mixture was stirred for 30 min at room temperature to give a red solution. Block like single crystals were formed at the bottom of the vessel after 3 days. The crystals were collected by filtration. Yield: 32 mg (64%). IR data (cm⁻¹): 1618, 1586, 1520, 1465, 1427, 1385, 1332, 1292, 1208, 1133, 1054, 953, 920, 841, 774, 726, 635, 600, 565, 532, 502, 460. UV-Vis (1.22×10⁻⁵ mol L⁻¹, MeOH; ε , L mol⁻¹ cm⁻¹): 250 (18,790), 260 (19,370), 312 (4,578), 400 (3,126). Anal. Calcd. (%) for $\rm C_{17}H_{14}Br_2N_2NiO_2$: C, 41.10; H, 2.84; N, 5.64. Found (%): C, 40.87; H, 2.90; N, 5.58.

2. 2. 2. $[Zn_3L_2(OAc)_2]$ (2)

 H_2L (44 mg, 0.10 mmol) and $Zn(CH_3COO)_2\cdot 2H_2O$ (44 mg, 0.20 mmol) were dissolved in methanol (30 mL). The mixture was stirred for 30 min at room temperature to give a colorless solution. Block like single crystals were formed at the bottom of the vessel after 6 days. The crystals were collected by filtration. Yield: 27 mg (45%). IR data

(cm⁻¹): 1636, 1583, 1525, 1459, 1421, 1385, 1275, 1193, 1175, 1073, 1038, 1004, 913, 859, 790, 732, 671, 617, 582, 508, 456. UV-Vis (1.36×10⁻⁵ mol L⁻¹, MeOH; ε , L mol⁻¹ cm⁻¹): 242 (20,520), 267 (10,455), 345 (5,380). Anal. Calcd. (%) for $C_{38}H_{32}Br_4N_4O_8Zn_3$: C, 38.40; H, 2.71; N, 4.71. Found (%): C, 38.53; H, 2.66; N, 4.78.

2. 2. 3. [ZnL(CH₃OH)] (3)

 $\rm H_2L$ (44 mg, 0.10 mmol) and ZnCl₂ (27 mg, 0.20 mmol) were dissolved in methanol (30 mL). The mixture was stirred for 30 min at room temperature to give a colorless solution. Needle like single crystals were formed at the bottom of the vessel after 2 days. The crystals were collected by filtration. Yield: 38 mg (70%). IR data (cm⁻¹): 1635, 1586, 1526, 1516, 1473, 1455, 1419, 1385, 1276, 1246, 1225, 1189, 1135, 1068, 1008, 985, 915, 859, 780, 732, 702, 601, 579, 553, 500, 454. UV-Vis (1.51×10⁻⁵ mol L⁻¹, MeOH; ε, L mol⁻¹ cm⁻¹): 230 (21,335), 246 (20,870), 272 (9,450), 348 (5,227). Anal. Calcd. (%) for $\rm C_{18}H_{18}Br_2N_2O_3Zn$: C, 40.37; H, 3.39; N, 5.23. Found (%): C, 40.18; H, 3.51; N, 5.16.

2. 2. 4. [MnClL(DMF)] (4)

 H_2L (44 mg, 0.10 mmol) and $MnCl_2 \cdot 2H_2O$ (40 mg, 0.20 mmol) were dissolved in methanol (30 mL). The mixture was stirred for 30 min at room temperature to give brown turbidity. Then, a few drops of DMF were added to give a clear solution. Block like single crystals were formed at the bottom of the vessel after 11 days. The crystals were

Table 1. Crystallographic data and refinement parameters for the complexes

	1	2	3	4
Chemical Formula	$C_{17}H_{14}Br_2N_2NiO_2$	C ₃₈ H ₃₂ Br ₄ N ₄ O ₈ Zn ₃	C ₁₈ H ₁₈ Br ₄ N ₂ O ₃ Zn	C ₂₀ H ₂₁ Br ₂ ClMnN ₃ O ₃
Fw	496.83	1188.42	535.53	601.61
Crystal system	Monoclinic	Monoclinic	Monoclinic	Monoclinic
Space group	$P2_1/c$	$P2_1/c$	$P2_1/n$	$P2_1/c$
a (Å)	11.3399(15)	17.197(2)	5.0165(12)	16.0852(16)
b (Å)	11.5440(15)	13.1073(15)	16.329(2)	11.3937(12)
c (Å)	12.8506(16)	21.815(2)	24.007(2)	12.5612(13)
a (°)	90	90	90	90
b (°)	98.049(2)	101.322(2)	91.828(2)	94.591(2)
g (°)	90	90	90	90
V (Å ³)	1665.7(4)	4821.5(9)	1965.5(6)	2294.7(4)
Z	4	4	4	4
m (Mo K α) (cm ⁻¹)	5.974	4.843	5.335	4.201
D_c (g cm ⁻³)	1.981	1.637	1.810	1.741
Reflections collected	8681	24362	10198	11879
Unique reflections	3091	8716	3642	4269
Observed reflections $[I \ge 2s(I)]$	2110	3603	2310	2551
Parameters	218	545	239	274
Restraints	18	62	19	0
Goodness of fit on F^2	1.122	0.976	1.023	1.005
R_1 , wR_2 $[I \ge 2s(I)]$	0.0598, 0.1341	0.0797, 0.1862	0.0586, 0.1255	0.0475, 0.1203
R_1 , wR_2 (all data)	0.0918, 0.1467	0.2000, 0.2561	0.1033, 0.1411	0.0986, 0.1540

collected by filtration. Yield: 23 mg (38%). IR data (cm⁻¹): 1677, 1633, 1586, 1522, 1459, 1417, 1385, 1320, 1276, 1202, 1135, 1068, 1040, 917, 856, 821, 790, 735, 685, 633, 593, 556, 512, 480, 470, 456, 427. UV-Vis (1.33×10⁻⁵ mol L⁻¹, MeOH; ε , L mol⁻¹ cm⁻¹): 210 (28,292), 245 (15,313), 280 (10,330), 315 (7,350), 405 (3,271). Anal. Calcd. (%) for $C_{20}H_{21}Br_2ClMnN_3O_3$: C, 39.93; H, 3.52; N, 6.98. Found (%): C, 40.15; H, 3.46; N, 7.07.

2. 3. X-ray Crystallography

Single crystal X-ray data for the complexes were collected on a Bruker SMART 1000 CCD diffractometer using SMART/SAINT.6 Intensity data were collected using graphite-monochromatized MoK_{α} radiation (0.71073 Å) at 298(2) K. Structures of the complexes were solved by direct methods using SHELX.7 Multi-scan absorption corrections were applied with SADABS.8 All non-hydrogen atoms were anisotropically treated. Atoms C8-C10 in complexes 1, 2 and 3, and atoms C25-C27 in complex 2 are slightly disordered, and were treated using restraints. The hydrogen atoms bonded to carbon were included in geometric positions and given thermal parameters equivalent to 1.2 and 1.5 times those of the atom to which they were attached. H5 atom in complex 4 was located from a difference Fourier map and refined with O-H distance restrained to 0.85(1) Å. The C8-C9-C10 group of complex 2 is disordered over two sites, with occupancies of 0.54(2) and 0.46(2), respectively. Crystallographic data and refinement parameters are given in Table 1, and important interatomic distances and angles are given in Table 2.

2. 4. Biological Assay

Antibacterial property of the compounds was evaluated by a macro-dilution method using *Staphylococcus aureus*, *Escherichia coli*, and *Candida parapsilosis*. The cultures of bacteria and yeast were incubated under vigorous shaking. The compounds were dissolved in small amounts of DMSO. Concentration of the tested compounds ranging from 0.010 to 2.5 mmol L⁻¹ for the bacteria and yeast was used in all experiments. Antibacterial activity was characterized by IC₅₀ and MIC values. MIC experiments on subculture dishes were used to assess the minimal microbicidal concentration (MMC). Subcultures were prepared separately in Petri dishes containing competent agar medium and incubated at 30 °C for 48 h. The MMC value was taken as the lowest concentration, which showed no visible growth of microbial colonies in the subculture dishes.

3. Results and Discussion

3. 1. Chemistry

Synthetic procedure for the complexes is shown in Scheme 2. Complex 1 was prepared by reaction of H₂L

Table 2. Selected bond distances (Å) and angles (°) for the complexes

		1	
Ni1-N1	1.822(7)	Ni1-N2	1.833(7)
Ni1-O1	1.829(5)	Ni1-O2	1.829(5)
N1-Ni1-O2	178.6(3)	N1-Ni1-O1	94.6(3)
O2-Ni1-O1	85.0(2)	N1-Ni1-N2	86.1(3)
O2-Ni1-N2	94.4(3)	O1-Ni1-N2	178.3(3)
		2	
Zn1-N1	2.041(10)	Zn1-N2	2.047(10)
Zn1-O6	1.980(8)	Zn1-O2	2.016(7)
Zn1-O1	2.030(7)	Zn2-O7	2.064(8)
Zn2-O5	2.084(8)	Zn2-O4	2.096(7)
Zn2-O1	2.103(7)	Zn2-O2	2.136(7)
Zn2-O3	2.145(7)	Zn3-O8	1.958(9)
Zn3-O4	2.001(7)	Zn3-N4	2.033(13)
Zn3-N3	2.043(12)	Zn3-O3	2.072(8)
O6-Zn1-O2	98.3(3)	O6-Zn1-O1	106.3(3)
O2-Zn1-O1	82.5(3)	O6-Zn1-N1	110.6(4)
O2-Zn1-N1	151.1(4)	O1-Zn1-N1	89.6(3)
O6-Zn1-N2	109.8(4)	O2-Zn1-N2	89.7(4)
O1-Zn1-N2	143.8(4)	N1-Zn1-N2	80.4(4)
O7-Zn2-O5	88.9(3)	O7-Zn2-O4	89.5(3)
O5-Zn2-O4	175.0(3)	O7-Zn2-O1	173.5(3)
O5-Zn2-O1	87.2(3)	O4-Zn2-O1	94.8(3)
O7-Zn2-O2	96.8(3)	O5-Zn2-O2	88.0(3)
O4-Zn2-O2	96.9(3)	O1-Zn2-O2	78.0(3)
O7-Zn2-O3	88.6(3)	O5-Zn2-O3	96.9(3)
O4-Zn2-O3	78.3(3)	O1-Zn2-O3	97.0(3)
O2-Zn2-O3	172.8(3)	O8-Zn3-O4	105.0(3)
O8-Zn3-N4	111.7(5)	O4-Zn3-N4	90.2(4)
O8-Zn3-N3	112.5(5)	O4-Zn3-N3	142.5(5)
N4-Zn3-N3	78.0(6)	O8-Zn3-O3	99.2(3)
O4-Zn3-O3	82.2(3)	N4-Zn3-O3	149.1(4)
N3-Zn3-O3	89.9(5)	144 ZII3 O3	147.1(4)
		3	
Zn1-O1	1.989(4)	Zn1-O2	1.964(5)
Zn1-O3	2.051(5)	Zn1-N1	2.091(6)
Zn1-N2	2.072(6)	2	2.071(0)
O2-Zn1-O1	94.4(2)	O2-Zn1-O3	100.4(2)
O1-Zn1-O3	100.8(2)	O2-Zn1-N2	89.4(2)
O1-Zn1-N2	150.8(3)	O3-Zn1-N2	107.0(3)
O2-Zn1-N1	157.0(3)	O1-Zn1-N1	88.1(2)
O3-Zn1-N1	101.6(2)	N2-Zn1-N1	77.8(3)
		4	
Mn1-O1	1.886(3)	Mn1-O2	1.901(4)
Mn1-N1	1.966(5)	Mn1-N2	1.983(5)
Mn1-O3	2.367(4)	Mn1-Cl1	2.4846(17)
O1-Mn1-O2	93.33(15)	O1-Mn1-N1	92.42(18)
O2-Mn1-N1	171.62(18)	O1-Mn1-N2	170.05(18)
O2-Mn1-N2	91.57(19)	N1-Mn1-N2	81.8(2)
O1-Mn1-O3	85.46(16)	O2-Mn1-O3	89.76(17)
N1-Mn1-O3	84.62(18)	N2-Mn1-O3	85.91(17)
O1-Mn1-Cl1	97.21(12)	O2-Mn1-Cl1	93.70(13)
N1-Mn1-Cl1	91.63(14)	N2-Mn1-Cl1	91.10(14)
	· · · · · · · · · · · · · · · · · ·	- · - · · · · · · · · · · · · · · · · ·	· -· - · (1 1 <i>)</i>
O3-Mn1-Cl1	175.50(12)		

with nickel acetate in methanol. Complex 2 was prepared by reaction of H_2L with zinc acetate in methanol. Although both complexes were synthesized from metal acetates, the acetate anion coordinates to the Zn atom in complex 2, while absent in complex 1. Complex 3 was prepared by reaction of H_2L with zinc chloride in methanol. Complex 4 was prepared by reaction of H_2L with manganese chloride in methanol and a few drops of DMF. The oxidation of Mn^{II} in manganese chloride was oxidized by air to Mn^{III} in the complex. Single crystals of the complexes were formed by slow evaporation of the solution in air.

Scheme 2. Synthetic procedure of the complexes.

3. 2. Crystal Structure Description of Complex 1

Molecular structure of complex 1 is shown in Fig. 1. The complex is a mononuclear nickel(II) species. The Ni atom is coordinated by two imine nitrogen and two phenolate oxygen of the Schiff base ligand, forming a square planar geometry. The cis and trans bond angles are $85.0(2)-94.6(3)^{\circ}$ and $178.6(3)-178.3(3)^{\circ}$, respectively. Thus, the square planar coordination is slightly distorted, which is

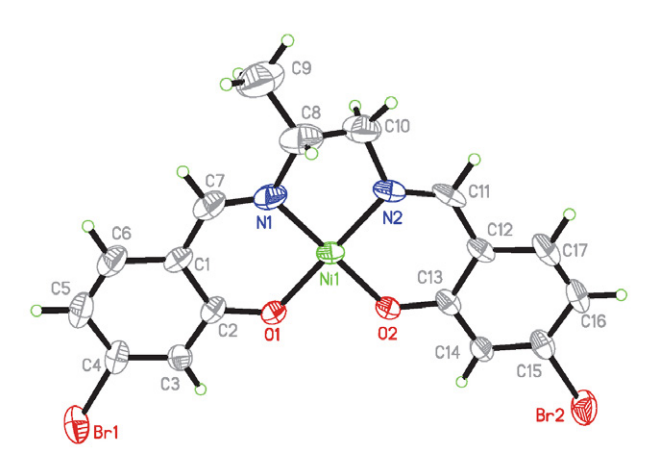


Fig. 1. A perspective view of the molecular structure of complex **1** with atom labeling scheme. Thermal ellipsoids are drawn at 30% probability level.

mainly caused by the five-membered chelate ring Ni1–N1–C8–C10–N2. The Ni–O and Ni–N bonds are 1.829(5) Å and 1.822(7)–1.833(7) Å, respectively, which are comparable to those observed in Schiff base nickel(II) complexes. The two benzene rings form a dihedral angle of 4.4(7)°.

3. 3. Crystal Structure Description of Complex 2

Molecular structure of complex 2 is shown in Fig. 2. The complex is a phenolate and acetate co-bridged trinuclear zinc(II) species. The Zn1...Zn2 and Zn2...Zn3 distances are 3.015(2) and 3.011(2) Å, respectively. The two outer Zn atoms (Zn1 and Zn3) are coordinated by two imine nitrogens (N1 and N2 for Zn1, N3 and N4 for Zn3) and two phenolate oxygens (O1 and O2 for Zn1, O3 and O4 for Zn3) of the Schiff base ligand in the basal plane, and by one acetate oxygen (O6 for Zn1, O8 for Zn3) at the apical position, forming square pyramidal geometry. The cis and trans bond angles in the basal planes are 80.4(4)-89.7(4)° and 143.8(4)-151.1(4)° for Zn1, and 78.0(6)-90.2(4)° and 142.5(5)-149.1(4)° for Zn3, respectively. The bond angles among apical and basal donor atoms are 98.3(3)-110.6(4)° for Zn1, and 99.2(3)–112.5(5)° for Zn3, respectively. Thus, the square pyramidal coordination is distorted, which is mainly caused by the strain created by the four-membered chelate rings Zn1-O1-Zn2-O2 and Zn2-O3-Zn3-O4, and the five-membered chelate rings Zn1-N1-C8-C9-N2 and Zn3-N3-C25-C26-N4. The inner Zn2 atom is coordinated by three phenolate oxygens (O1, O2, O3) from two Schiff base ligands and one acetate oxygen (O7) of an acetate ligand in the equatorial plane, and by one phenolate oxygen (O4) of a Schiff base ligand and one acetate oxygen (O5) at the axial positions, forming octahedral geometry.

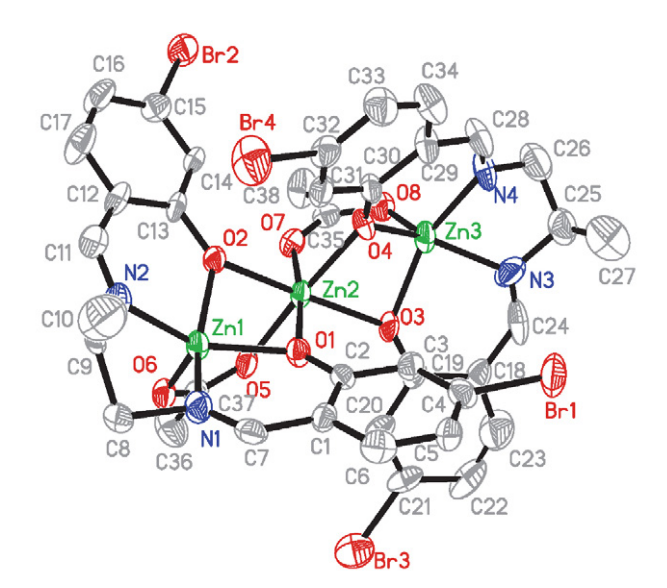


Fig. 2. A perspective view of the molecular structure of complex **2** with atom labeling scheme. Thermal ellipsoids are drawn at 30% probability level. H-atoms were omitted for clarity.

The *cis* and *trans* bond angles in the equatorial plane are 78.0(3)–97.0(3)° and 172.8(3)–173.5(3)°, respectively. The bond angles among axial and equatorial donor atoms are 78.3(3)–96.9(3)°. The bond angle between two axial donor atoms is 175.0(3)°. Thus, the octahedral coordination is slightly distorted. The Zn–O and Zn–N bonds are 1.958(9)–2.145(7) Å and 2.033(13)–2.047(10) Å, respectively, which are comparable to those observed in other Schiff base zinc(II) complexes.¹⁰ The two benzene rings of the Schiff base ligands form dihedral angles of 42.4(6) and 46.2(6)°.

3. 4. Crystal Structure Description of Complex 3

Molecular structure of complex 3 is shown in Fig. 3. The complex is a mononuclear zinc(II) species. The Zn atom is coordinated by two imine nitrogens (N1 and N2) and two phenolate oxygens (O1 and O2) of the Schiff base ligand in the basal plane, and by one oxygen (O3) of a methanol ligand at the apical position, forming square pyramidal geometry. The *cis* and *trans* bond angles in the basal plane are 77.8(3)–94.4(2)° and 150.8(3)–157.0(3)°, respectively. The bond angles among apical and basal do-

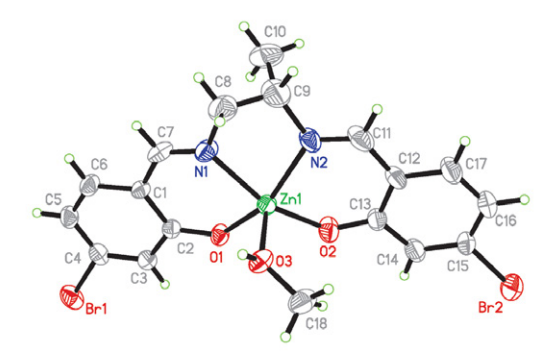


Fig. 3. A perspective view of the molecular structure of complex **3** with atom labeling scheme. Thermal ellipsoids are drawn at 30% probability level.

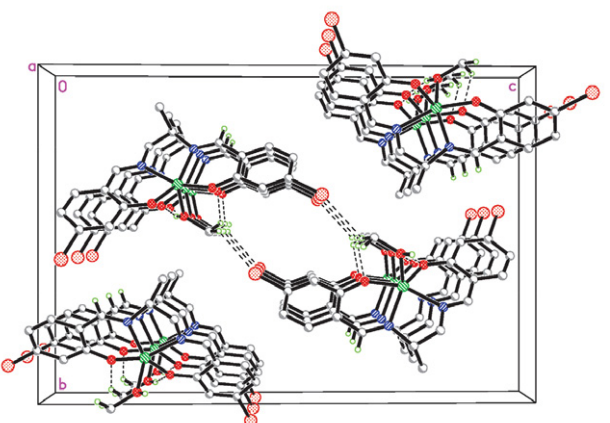


Fig. 4. Molecular packing diagram of complex **3**, viewed along *a* axis. Hydrogen bonds are shown as dashed lines.

nor atoms are 100.8(2)–107.0(3)°. Thus, the square pyramidal coordination is distorted, which is mainly caused by the strain created by the four-membered chelate ring Zn1–N1–C8–C9–N2. The Zn–O and Zn–N bonds are 1.964(5)–2.091(6) Å and 2.072(6)–2.091(6) Å, respectively, which are comparable to those observed in complex 2 and other Schiff base zinc(II) complexes. The two benzene rings of the Schiff base ligand form dihedral angle of 6.0(3)°. In the crystal structure, molecules are linked through intermolecular hydrogen bonds of C-H···Br, to form dimers (Fig. 4).

3. 5. Crystal Structure Description of Complex 4

Molecular structure of complex 4 is shown in Fig. 5. The complex is a mononuclear manganese(III) species. The Mn atom is coordinated by two imine nitrogens (N1 and N2) and two phenolate oxygens (O1 and O2) of the Schiff base ligand in the equatorial plane, and by one oxygen (O3) of a DMF ligand and one Cl atom at the axial positions, forming octahedral geometry. The cis and trans bond angles in the equatorial plane are 81.8(2)-93.33(15)° and 170.05(18)-171.62(18)°, respectively. The bond angles among axial and equatorial donor atoms are 84.62(18)-97.21(12)°. The bond angle between two axial donor atom is 175.50(12)°. Thus, the octahedral coordination is slightly distorted, which is mainly caused by the strain created by the five-membered chelate ring Mn1-N1-C8-C9-N2. The Mn-O and Mn-N bonds are 1.886(3)-2.367(4) Å and 1.966(5)-1.983(5) Å, respectively, which are comparable to those observed in other Schiff base manganese(III) complexes.¹¹ The two benzene rings of the Schiff base ligand form dihedral angle of 7.6(5)°. In the crystal structure, molecules are linked through intermolecular hydrogen bonds of C-H...Cl, to form chains along c axis (Fig. 6).

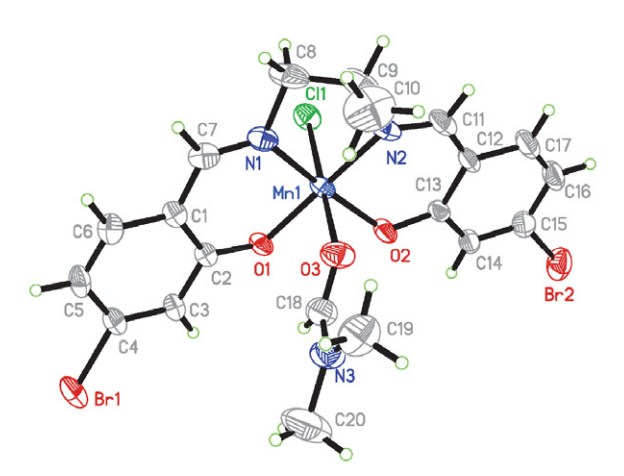


Fig. 5. A perspective view of the molecular structure of complex **4** with atom labeling scheme. Thermal ellipsoids are drawn at 30% probability level.

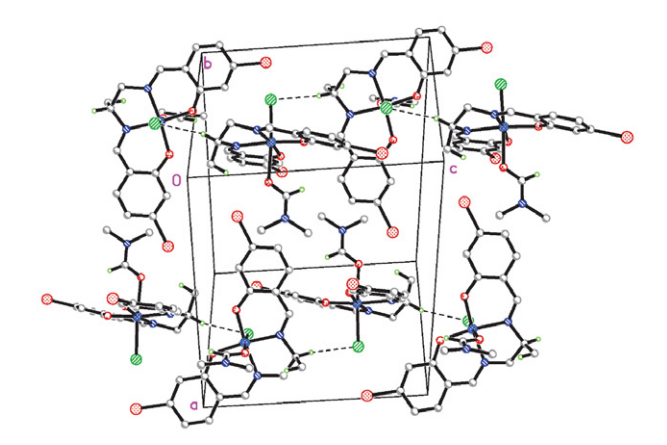


Fig. 6. Molecular packing diagram of complex **4**, viewed along *a* axis. Hydrogen bonds are shown as dashed lines.

Table 3. Geometrical parameters for hydrogen bonds for complexes

D-H···A		Angle		
	D-H	HA	DA	D-H···A,°
3				
C18-H18A···O2i	0.96	2.42	3.212(10)	140(6)
O3-H3···O1 ⁱ	0.85(1)	1.81(3)	2.636(7)	165(9)
4				
C9-H9···Cl1 ⁱⁱ	0.98	2.74	3.686(7)	163(7)

Symmetry codes: i) 1 + x, y, z; (ii) x, $1\frac{1}{2} - y$, $\frac{1}{2} + z$.

3. 6. IR and UV-Vis Spectra

In the infrared spectra of the compounds, the strong absorption band at $1623~\rm cm^{-1}$ for $\rm H_2L$ is assigned to the azomethine groups, $\nu(\rm C=N)$, which is shifted to higher wave numbers 1633- $1636~\rm cm^{-1}$ for the complexes. IR spectrum of complex 4 displays characteristic band of carbonyl group at $1677~\rm cm^{-1}$ for DMF ligand. The weak bands in low wave numbers 400– $600~\rm cm^{-1}$ are due to the vibration of M–O, M–N and M–Cl bonds. 12

In the electronic spectra of the compounds, the intense bands observed at 230–250 nm are assigned to intra-ligand π – π * transitions. The bands at 260–350 nm are

assigned to intra-ligand $n-\pi^*$ transitions. The nickel and manganese complexes displayed bands centered at 400 and 405 nm, which can be assigned to d-d transition.

3. 7. Antibacterial Activity

The antimicrobial results are summarized in Table 4. The free Schiff base H₂L showed medium activity against E. coli, while there was no activity on S. aureus and C. parapsilosis. The nickel complex has similar activity against the bacteria strains as compared to H₂L. Obviously, the two zinc complexes have stronger activity than H₂L. Both zinc complexes showed strong activity against S. aureus and E. coli, and medium activity against C. parapsilosis. The manganese complex has weak or no activity against the bacteria and yeast. Interestingly, complexes 2 and 3 have the most activity against S. aureus, with IC₅₀ and MIC values of 0.26-0.32 and 0.31 mmol L⁻¹, which deserves further study. As a comparison, the two zinc complexes have similar antibacterial activities against S. aureus and E. coli to the Schiff base copper(II) complexes.^{5,13} The two zinc complexes have similar activities against S. aureus and E. coli as compared with ciprofloxacin, but the nickel and manganese complexes are much weaker.

4. Conclusion

In summary, four new nickel, zinc and manganese complexes with the Schiff base ligand *N*,*N*'-bis(4-bromosalicylidene)propane-1,2-diamine were prepared. Structures of the complexes were characterized by IR, UV-Vis spectra, and confirmed by single crystal X-ray determination. The Schiff base ligand coordinates to the metal atoms through the phenolate oxygen and imine nitrogen. The two zinc complexes have effective antibacterial activities on the bacteria *Staphylococcus aureus* and *Escherichia coli*, and yeast *Candida parapsilosis*.

Supplementary Material

CCDC 2411111–2411114 contain the supplementary crystallographic data for this paper. These data can be

Table 4. Antibacterial activity of the compounds

Compound	S. aureus		E. coli		C. parapsilosis	
-	${\rm IC_{50}}^*$	\mathbf{MIC}^*	IC_{50}	MIC	IC_{50}	MIC
$\overline{\mathrm{H_2L}}$	>2.50	>2.50	1.45	2.50	>2.50	>2.50
1	>2.50	>2.50	1.27	2.50	>2.50	>2.50
2	0.26	0.31	0.72	0.63	1.51	1.25
3	0.32	0.31	0.87	0.63	2.15	2.50
4	>2.50	>2.50	>2.50	>2.50	>2.50	>2.50
Ciprofloxacin	0.23	0.16	0.36	0.31	0.54	0.62

^{*} mmol L-1

obtained free of charge at http://www.ccdc.cam.ac.uk/const/retrieving.html or from the Cambridge Crystallographic Data Centre, 12 Union Road, Cambridge CB2 1EZ, UK; fax: +44(0)1223-336033 or email: deposit@ccdc.cam.ac.uk.

5. References

- (a) P. Bhunia, S. Dutta, S. Maity, J. Mayans, A. Escuer, A. Ghosh, *Inorg. Chim. Acta* 2023, 545, 121264;
 - DOI:10.1016/j.ica.2022.121264
 - (b) A. Ajaz, M. A. Shaheen, M. Ahmed, K. S. Munawar, A. Siddique, A. Karim, N. Ahmad, M. F. U. Rehman, *RSC Advances* **2023**, *13*, 2756–2767; **DOI**:10.1039/D2RA07051K
 - (c) P. Middya, D. Roy, S. Chattopadhyay, *Inorg. Chim. Acta* **2023**, *548*, 121377; **DOI:**10.1016/j.ica.2023.121377
 - (d) M. Abdi, A. F. Shojaei, M. Ghadermazi, Z. Moradi-Shoeili, *Acta Chim. Slov.* **2020**, *67*, 476–486;

DOI:10.17344/acsi.2019.5466

- (e) L.-W. Xue, Q.-L. Peng, P.-P. Wang, H.-J. Zhang, *Acta Chim. Slov.* **2019**, *66*, 694–700; **DOI:**10.17344/acsi.2019.5151
- (f) C.-L. Zhang, X.-Y. Qiu, S.-J. Liu, *Acta Chim. Slov.* **2019**, *66*, 484–489. **DOI**:10.17344/acsi.2019.5019
- (a) N. A. A. Elkanzi, H. Hrichi, H. Salah, M. Albqmi, A. M. Ali, A. Abdou, *Polyhedron* 2023, 230, 116219;

DOI:10.1016/j.poly.2022.116219

- (b) S. K. Patel, K. Kolte, C. J. Savani, P. Raghavaiah, D. Dave, A. A. Isab, D. Mistry, D. Suthar, V. K. Singh, *Inorg. Chim. Acta* **2022**, *543*, 121139; **DOI**:10.1016/j.ica.2022.121139
- (c) A. Ali, M. Pervaiz, Z. Saeed, U. Younas, R. Bashir, S. Ullah, S. M. Bukhari, F. Ali, S. Jelani, A. Rashid, A. Adnan, *Inorg. Chem. Commun.* **2022**, *145*, 109903;

DOI:10.1016/j.inoche.2022.109903

- (d) D.-L. Peng, N. Sun, *Acta Chim. Slov.* **2018**, *65*, 895–901; **DOI**:10.17344/acsi.2018.4543
- (e) G.-X. He, L.-W. Xue, Q.-L. Peng, P.-P. Wang, H.-J. Zhang, *Acta Chim. Slov.* **2019**, *66*, 570–575.

DOI:10.17344/acsi.2018.4868

- (a) S. Mandal, T. Sen, U. Mandal, D. Bhunia, C. Rizzoli, D. Bandyopadhyay, *J. Coord. Chem.* 2019, 72, 3614–3624;
 DOI:10.1080/00958972.2019.1704275
 - (b) H. Keypour, F. Forouzandeh, S. Salehzadeh, F. Hajibabaei, S. Feizi, R. Karamian, N. Ghiasi, R. W. Gable, *Polyhedron* **2019**, *170*, 584–592; **DOI**:10.1016/j.poly.2019.06.023
 - (c) H. Y. Qian, N. Sun, *Transition Met. Chem.* **2019**, 44, 501–506; **DOI**:10.1007/s11243-018-00296-x
 - (d) M. H. Esfahani, H. Iranmanesh, J. E. Beves, M. Kaur, J. P. Jasinski, M. Behzad, *J. Coord. Chem.* **2019**, *72*, 2326–2336. **DOI**:10.1080/00958972.2019.1643846
- 4. (a) P. Middya, P. Chakraborty, S. Chattopadhyay, *Inorg. Chim. Acta* 2023, 552, 121479; DOI:10.1016/j.ica.2023.121479
 (b) K.-S. Cao, L.-W. Xue, Q.-R. Liu, *Acta Chim. Slov.* 2023, 70, 516–523; DOI:10.17344/acsi.2023.8359
 - (c) Y.Y. Luo, J.Q. Wang, B.T. Zhang, Y.X. Guan, T. Yang, X.Y. Li, L.Y. Xu, J. Wang, Z.L. You, J. Coord. Chem. **2020**, 73, 1765–

- 1777; **DOI:**10.1080/00958972.2020.1795645
- (d) J.-L. Hou, H.-Y. Wu, C.-B. Sun, Y. Bi, W. Chen, *Acta Chim. Slov.* **2020**, *67*, 860–865; **DOI:**10.17344/acsi.2020.5824
- (e) M. Nejadmirfathi, M. Montazerozohori, R. Naghiha, E.P. Kokhdan, S. Hosseinifar, *Inorg. Chem. Commun.* **2024**, *161*, 111991; **DOI**:10.1016/j.inoche.2023.111991
- (f) S. Batool, Imtiaz-Ud-Din, A. Zafar, M. Athar, M. Mehmood, M.N. Tahir, I.U. Haq, S.S. Azam, *J. Coord. Chem.* **2023**, *76*, 1189–1213; **DOI**:10.1080/00958972.2023.2230607
- (g) B. Archana, S. Sreedaran, *Polyhedron* **2023**, *231*, 116269; **DOI**:10.1016/j.poly.2022.116269
- (h) P. Paul, K.R.N. Bhowmik, S. Roy, D. Deb, N. Das, M. Bhattacharjee, R.N.D. Purkayastha, L. Male, V. Mckee, R. Pallepogu, D. Maiti, A. Bauza, A. Fontera, A.M. Kirillov, *Polyhedron* **2018**, *151*, 407–416. **DOI:**10.1016/j.poly.2018.05.043
- Y.-M. Hao, Acta Chim. Slov. 2023, 70, 327–332.
 DOI:10.17344/acsi.2023.8104
- SMART/SAINT, Madison (WI, USA): Bruker AXS, Inc., 2004
- 7. G. M. Sheldrick, Acta Crystallogr. 2015, C71, 3-11.
- 8. G. M. Sheldrick, *SADABS*, Göttingen (Germany): Univ. of Göttingen, **1999**.
- (a) M. Kondo, K. Nabari, T. Horiba, Y. Irie, Md.K. Kabir, R.P. Sarker, E. Shimizu, Y. Shimizu, Y. Fuwa, *Inorg. Chem. Commun.* 2003, 6, 154–156;

DOI:10.1016/S1387-7003(02)00708-6

- (b) Y. Shimazaki, T. Yajima, F. Tani, S. Karasawa, K. Kukui, Y. Naruta, O. Yamauchi, *J. Am. Chem. Soc.* **2007**, *129*, 2559–2568; **DOI**:10.1021/ja067022r
- (c) S. Fritzsche, P. Lonnecke, T. Hocher, E. Hey-Hawkins, *Z. Anorg. Allg. Chem.* **2006**, 632, 2256–2267.

DOI:10.1002/zaac.200600155

- (a) A. Sarnicka, P. Starynowicz, J. Lisowski, *Chem. Commun.* 2012, 48, 2237–2239; DOI:10.1039/c2cc16673a
 - (b) B. Dutta, P. Bag, U. Florke, K. Nag, *Inorg. Chem.* **2005**, *44*, 147–157; **DOI**:10.1021/ic049056a
 - (c) X.-X. Zhou, H.-C. Fang, Y.-Y. Ge, Z.-Y. Zhou, Z.-G. Gu, X. Gong, G. Zhao, Q.-G. Zhan, R.-H. Zeng, Y.-P. Cai, *Cryst. Growth Des.* **2010**, *10*, 4014–4022. **DOI:**10.1021/cg100612b
- (a) C.-H. Li, K.-L. Huang, J.-M. Dou, Y.-N. Chi, Y.-Q. Xu,
 L. Shen, D.-Q. Wang, C.-W. Hu, Cryst. Growth Des. 2008, 8,
 3141–3143; DOI:10.1021/cg800504a
 - (b) P. Chakraborty, S. Majumder, A. Jana, S. Mohanta, *Inorg. Chim. Acta* **2014**, *410*, 65–75;

DOI:10.1016/j.ica.2013.10.013

- (c) M.R. Bermejo, A. Castineiras, J.C. Garcia-Monteagudo, M. Rey, A. Sousa, M. Watkinson, C.A. McAuliffe, R.G. Pritchard, R.L. Beddoes, *J. Chem. Soc., Dalton Trans.* **1996**, 2935–2944. **DOI**:10.1039/DT9960002935
- A. Ray, D. Sadhukhan, G. Rosair, C. J. Gomez-Garcia, S. Mitra, *Polyhedron* 2009, 28, 3542–3550.
 DOI:10.1016/j.poly.2009.07.017
- 13. Y.-M. Hao, Russ. J. Coord. Chem. **2015**, 41, 25–30. **DOI:**10.1134/S1070328415010030

Povzetek

Sintetizirali smo štirje nove komplekse niklja(II), cinka(II) in mangana(III), [NiL] (1), [Zn₃L₂(OAc)₂] (2), [ZnL(CH₃OH)] (3) in [MnClL(DMF)] (4), z ligandom bis-Schiffove baze N,N'-bis(4-bromosaliciliden)propan-1,2-diamin (H₂L) in jih okarakterizirali s spektroskopskimi metodami ter z rentgensko strukturno analizo. Atom Ni v enojedrnem nikljevem kompleksu 1 ima kvadratno planarno koordinacijo. Zunanji in notranji atom Zn v trinuklearnem cinkovem kompleksu 2 imajo kvadratno planarno oziroma oktaedrično koordinacijo. Atom Zn v enojedrnem cinkovem kompleksu 3 ima kvadratno piramidalno koordinacijo. Atom Mn v enojedrnem manganovem kompleksu 4 ima oktaedrično koordinacijo. Antibakterijsko aktivnost kompleksov smo preverili na bakterijah Staphylococcus aureus in Escherichia coli ter kvasovkah Candida parapsilosis.



Except when otherwise noted, articles in this journal are published under the terms and conditions of the Creative Commons Attribution 4.0 International License